nature physics

ARTICLES

PUBLISHED ONLINE: 28 FEBRUARY 2010 | DOI: 10.1038/NPHYS1535

Two-orbital *SU(N)* magnetism with ultracold alkaline-earth atoms

A. V. Gorshkov[1]*, M. Hermele[2], V. Gurarie[2], C. Xu[1], P. S. Julienne[3], J. Ye[4], P. Zoller[5,6], E. Demler[1,7], M. D. Lukin[1,7] and A. M. Rey[4]

Fermionic alkaline-earth atoms have unique properties that make them attractive candidates for the realization of atomic clocks and degenerate quantum gases. At the same time, they are attracting considerable theoretical attention in the context of quantum information processing. Here we demonstrate that when such atoms are loaded in optical lattices, they can be used as quantum simulators of unique many-body phenomena. In particular, we show that the decoupling of the nuclear spin from the electronic angular momentum can be used to implement many-body systems with an unprecedented degree of symmetry, characterized by the *SU(N)* group with *N* as large as 10. Moreover, the interplay of the nuclear spin with the electronic degree of freedom provided by a stable optically excited state should enable the study of physics governed by the spin–orbital interaction. Such systems may provide valuable insights into the physics of strongly correlated transition-metal oxides, heavy-fermion materials and spin-liquid phases.

The interest in fermionic alkaline-earth atoms[1–8] stems from their two key features: (1) the presence of a metastable excited state $^3P_0$ coupled to the ground $^1S_0$ state through an ultranarrow doubly forbidden transition[1] and (2) the almost perfect decoupling[1] of the nuclear spin I from the electronic angular momentum J in these two states, because they both have $J=0$. This decoupling implies that s-wave scattering lengths involving states $^1S_0$ and $^3P_0$ are independent of the nuclear spin, aside from the restrictions imposed by fermionic antisymmetry. We show that the resulting $SU(N)$ spin symmetry (where $N=2I+1$ can be as large as 10) together with the possibility of combining (nuclear) spin physics with (electronic) orbital physics opens up a wide field of rich many-body systems with alkaline-earth atoms.

In what follows, we derive the two-orbital $SU(N)$-symmetric Hubbard model describing alkaline-earth atoms in $^1S_0$ and $^3P_0$ states trapped in an optical lattice. We focus on specific parameter regimes characterized by full or partial atom localization resulting from strong atomic interactions, where simpler effective spin Hamiltonians can be derived. The interplay between orbital and spin degrees of freedom in such effective models is a central topic in quantum magnetism and has attracted wide interest in the condensed-matter community. Alkaline-earth atoms thus provide, on the one hand, a unique opportunity for the implementation of some of these models for the first time in a defect-free and fully controllable environment. On the other hand, they open a new arena to study a wide range of models, many of which have not been discussed previously, even theoretically. We demonstrate, in particular, how to implement the Kugel–Khomskii model studied in the context of transition-metal oxides[9–13], the Kondo lattice model[14–26] (KLM) studied in the context of manganese oxide perovskites[20] and heavy-fermion materials[25], as well as various $SU(N)$-symmetric spin Hamiltonians that are believed to have spin-liquid and valence-bond-solid (VBS) ground states[27–34]. For example, we discuss how, by appropriately choosing the initial state, a single alkaline-earth atom species with $I=9/2$ (such as ^{87}Sr) can be used to study experimentally such a distinctively theoretical object as the phase diagram as a function of N for all $N\leq 10$.

Before proceeding, we note that, whereas an orthogonal symmetry group SO(5) can be realized in alkali atoms[35], proposals to obtain $SU(N>2)$-symmetric models with alkali atoms[36,37] and solid-state systems[11,38] are a substantial idealization owing to strong hyperfine coupling and a complex solid-state environment, respectively. In this context, alkaline-earth-like atoms make an exceptional system to study models with $SU(N>2)$ symmetry.

Alkaline-earth atoms in an optical lattice

We begin with the Hamiltonian (H) describing cold fermionic alkaline-earth atoms in an external trapping potential:

$$\begin{aligned} H &= \sum_{\alpha m}\int \mathrm{d}^3\mathbf{r}\,\Psi^\dagger_{\alpha m}(\mathbf{r})\left(-\frac{\hbar^2}{2M}\nabla^2+V_\alpha(\mathbf{r})\right)\Psi_{\alpha m}(\mathbf{r}) \\ &+\hbar\omega_0\int \mathrm{d}^3\mathbf{r}(\rho_e(\mathbf{r})-\rho_g(\mathbf{r}))+\frac{g^+_{eg}+g^-_{eg}}{2}\int \mathrm{d}^3\mathbf{r}\rho_e(\mathbf{r})\rho_g(\mathbf{r}) \\ &+\sum_{\alpha,m<m'} g_{\alpha\alpha}\int \mathrm{d}^3\mathbf{r}\rho_{\alpha m}(\mathbf{r})\rho_{\alpha m'}(\mathbf{r}) \\ &+\frac{g^+_{eg}-g^-_{eg}}{2}\sum_{mm'}\int \mathrm{d}^3\mathbf{r}\,\Psi^\dagger_{gm}(\mathbf{r})\,\Psi^\dagger_{em'}(\mathbf{r})\,\Psi_{gm'}(\mathbf{r})\,\Psi_{em}(\mathbf{r}) \end{aligned} \quad (1)$$

Here $\Psi_{\alpha m}(\mathbf{r})$ is a fermion field operator for atoms in internal state $|\alpha m\rangle$, where $\alpha=g$ ($^1S_0$) or e ($^3P_0$) denotes the electronic state and $m=-I,\ldots,I$ denotes one of the $N=2I+1$ nuclear Zeeman states.

[1]Physics Department, Harvard University, Cambridge, Massachusetts 02138, USA, [2]Department of Physics, University of Colorado, Boulder, Colorado 80309, USA, [3]Joint Quantum Institute, NIST and University of Maryland, Gaithersburg, Maryland 20899-8423, USA, [4]JILA, NIST, and Department of Physics, University of Colorado, Boulder, Colorado 80309, USA, [5]Institute for Theoretical Physics, University of Innsbruck, A-6020 Innsbruck, Austria, [6]Institute for Quantum Optics and Quantum Information of the Austrian Academy of Sciences, A-6020 Innsbruck, Austria, [7]Institute for Theoretical Atomic, Molecular and Optical Physics, Harvard–Smithsonian Center of Astrophysics, Cambridge, Massachusetts 02138, USA.
*e-mail: gorshkov@post.harvard.edu.

The density operators are defined as $\rho_{\alpha m}(\mathbf{r}) = \Psi^{\dagger}_{\alpha m}(\mathbf{r})\Psi_{\alpha m}(\mathbf{r})$ and $\rho_{\alpha}(\mathbf{r}) = \sum_m \rho_{\alpha m}(\mathbf{r})$. The term $V_{\alpha}(\mathbf{r})$ describes the external trapping potential, which we will assume to be an optical lattice independent of the nuclear spin: even for a relatively deep lattice with a 100 kHz trap frequency, tensor and vector light shifts should be well below 1 Hz (ref. 1). $\hbar\omega_0$ is the transition energy between $|g\rangle$ and $|e\rangle$, where $\hbar$ is the reduced Plank's constant and ω is the frequency. Extra lasers can be used to drive transitions between $|g\rangle$ and $|e\rangle$ levels[1,2]. As we will need these extra lasers only for system preparation, we have not included the corresponding terms in the Hamiltonian.

The interaction is characterized by four s-wave scattering lengths a_X, $X = gg, ee, eg^+, eg^-$, which define four interaction parameters $g_X = 4\pi\hbar^2 a_X/M$, where M is atomic mass. a_{gg}, a_{ee} and $a^{\pm}_{eg}$ are the scattering lengths for two atoms in the electronic state $|gg\rangle$, $|ee\rangle$ and $|\pm\rangle = (|ge\rangle \pm |eg\rangle)/\sqrt{2}$, respectively. As shown in Fig. 1, the fermionic antisymmetry then forces the nuclear state to be symmetric for the only antisymmetric electronic state $|-\rangle$ and antisymmetric otherwise. Very few a_X are known at the moment (see Supplementary Information).

The independence of each of the four scattering lengths from the nuclear spin state is essential to the fulfilment of the $SU(N)$ symmetry of our model (see the Symmetries of the Hamiltonian section). This independence is a consequence of the decoupling between nuclear and electronic degrees of freedom shown during the course of a collision involving any combination of g or e states, which both have $J = 0$. Although for the $|e\rangle \equiv {}^3P_0$ atom, the decoupling is slightly broken by the admixture with higher-lying P states with $J \neq 0$, this admixture is very small[1] and the resulting nuclear-spin-dependent variation of the scattering lengths is also expected to be very small, of the order of 10^{-3} (see Supplementary Information). For a_{gg}, which does not involve state $|e\rangle$, this variation should be even smaller ($\sim 10^{-9}$).

The interaction terms in equation (1) describe the most general s-wave two-body interaction consistent with elastic collisions as far as the electronic state is concerned and with the independence of the scattering length from the nuclear spin. Whereas the assumption of elasticity for g–g and e–g collisions is well justified, because no inelastic exit channels exist, e–e collisions are likely to be accompanied by large losses, which means that the magnitudes of the imaginary and real parts of the e–e scattering length are likely to be comparable (see Supplementary Information). Therefore, we focus below on those situations where two e atoms never occupy the same site.

We assume that only the lowest band in both e and g lattices is occupied and expand the field operators in terms of the corresponding (real) Wannier basis functions $\Psi_{\alpha m}(\mathbf{r}) = \sum_j w_{\alpha}(\mathbf{r} - \mathbf{r}_j)c_{j\alpha m}$, where $c^{\dagger}_{j\alpha m}$ creates an atom in internal state $|\alpha m\rangle$ at site j (centred at position $\mathbf{r}_j$). Equation (1) reduces then to a two-orbital single-band Hubbard Hamiltonian

$$H = -\sum_{\langle j,i\rangle\alpha,m} J_{\alpha}(c^{\dagger}_{i\alpha m}c_{j\alpha m} + \text{h.c.}) + \sum_{j,\alpha}\frac{U_{\alpha\alpha}}{2}n_{j\alpha}(n_{j\alpha}-1) + V\sum_j n_{je}n_{jg} + V_{ex}\sum_{j,m,m'} c^{\dagger}_{jgm}c^{\dagger}_{jem'}c_{jgm'}c_{jem} \quad (2)$$

Here $J_{\alpha} = -\int \mathrm{d}^3\mathbf{r} w_{\alpha}(\mathbf{r})(-(\hbar^2/2M)\nabla^2 + V_{\alpha}(\mathbf{r}))w_{\alpha}(\mathbf{r} - \mathbf{r}_0)$ are the tunnelling energies, $\mathbf{r}_0$ connects two nearest neighbours, h.c. stands for Hermitian conjugate, $n_{j\alpha m} = c^{\dagger}_{j\alpha m}c_{j\alpha m}$ and $n_{j\alpha} = \sum_m n_{j\alpha m}$. The tunnelling is isotropic, which is a crucial difference between this model and its analogues in solid-state systems with orbital degeneracy[9]. The sum $\langle j, i\rangle$ is over pairs of nearest-neighbour sites i, j. $V = (U^+_{eg} + U^-_{eg})/2$ and $V_{ex} = (U^+_{eg} - U^-_{eg})/2$ describe the direct and exchange interaction terms, respectively. The onsite interaction energies are $U_{\alpha\alpha} = g_{\alpha\alpha}\int \mathrm{d}^3\mathbf{r} w^4_{\alpha}(\mathbf{r})$ and $U^{\pm}_{eg} = g^{\pm}_{eg}\int \mathrm{d}^3\mathbf{r} w^2_e(\mathbf{r})w^2_g(\mathbf{r})$. Constant terms, proportional to $\sum_j n_{j\alpha}$, are omitted in equation (2).

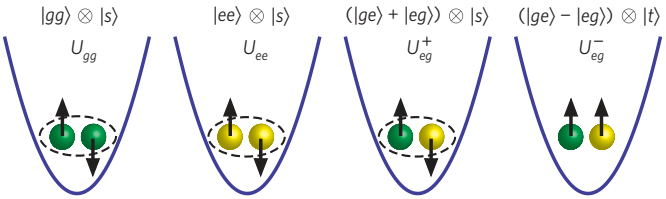

Figure 1 | Interaction parameters between *g* and *e* atoms loaded in the lowest vibrational state of the corresponding optical lattice. Green spheres: g atoms; yellow spheres: e atoms. Here we assumed the nuclear spin to be $I = 1/2$, and the arrows indicate the $m_I = \pm 1/2$ spin states. $|s, t\rangle$ denote the singlet and triplet nuclear spin states of the two atoms (only one of three triplet states—$|\uparrow\uparrow\rangle$—is shown). The dashed ellipse represents antisymmetrization of the nuclear spin state (that is, $|s\rangle$). The interaction energy U_X ($X = gg, ee, eg^+, eg^-$) is proportional to the corresponding scattering length a_X.

Experimental control over the parameters in equation (2) will enable us to manipulate the atoms (see the Methods section).

Symmetries of the Hamiltonian

To understand the properties of the Hamiltonian in equation (2), we consider its symmetries. We define $SU(2)$ pseudo-spin algebra

$$T^{\mu} = \sum_j T^{\mu}_j = \frac{1}{2}\sum_{jm\alpha\beta} c^{\dagger}_{j\alpha m}\sigma^{\mu}_{\alpha\beta}c_{j\beta m}$$

where σ^{μ} ($\mu = x, y, z$) are Pauli matrices in the $\{e, g\}$ basis. We further define nuclear-spin permutation operators

$$S^m_n = \sum_j S^m_n(j) = \sum_{j,\alpha} S^m_n(j,\alpha) = \sum_{j,\alpha} c^{\dagger}_{j\alpha n}c_{j\alpha m}$$

which satisfy the $SU(N)$ algebra $[S^m_n, S^p_q] = \delta_{mq}S^p_n - \delta_{pn}S^m_q$ and thus generate $SU(N)$ rotations of nuclear spins ($N = 2I + 1$).

In addition to the obvious conservation of the total number of atoms $n = \sum_j (n_{je} + n_{jg})$, H shows $U(1) \times SU(N)$ symmetry (see the Methods section for the discussion of enhanced symmetries), where $U(1)$ is associated with the elasticity of collisions as far as the electronic state is concerned ($[T^z, H] = 0$) and $SU(N)$ is associated with the independence of scattering and of the trapping potential from the nuclear spin ($[S^m_n, H] = 0$ for all n, m). The two-orbital $SU(N)$-symmetric Hubbard Hamiltonian in equation (2) is a generalization to $N > 2$ of its $SU(2)$-symmetric counterpart[9] and to two orbitals of its single-orbital counterpart[28]. The $SU(N)$ symmetry and the largely independent spin and orbital degrees of freedom are two unique features present in alkaline earths but absent in alkalis owing to strong hyperfine interactions.

One important consequence of $SU(N)$ symmetry is the conservation, for any m, of S^m_m, the total number of atoms with nuclear spin m. This means that an atom with large I, for example, ^{87}Sr ($I = 9/2$), can reproduce the dynamics of atoms with lower I if one takes an initial state with $S^m_m = 0$ for some m values. To verify $SU(N)$ symmetry of the interaction experimentally, one could, thus, put two atoms in one well in spins m and m' and confirm that collisions do not populate other spin levels. This feature of $SU(N)$ symmetry is in stark contrast to the case of weaker $SU(2)$ symmetry, where the dependence of scattering lengths on the total spin of the two colliding particles allows for scattering into spin states other than m and m'. We note that although collisions are governed by electronic interactions and obey the nuclear-spin $SU(N)$ symmetry, the nuclear spins still indirectly control the collisions through fermionic statistics and give rise to effective spin–orbital and spin–spin interactions.

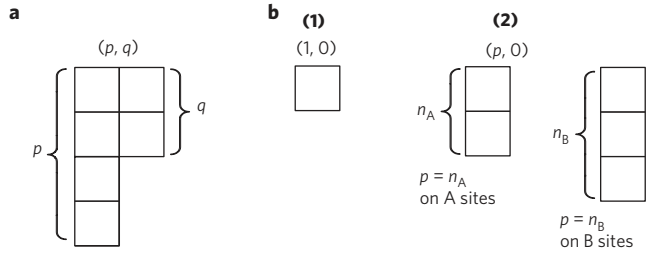

Figure 2 | Young diagrams describing the irreducible representations of *SU(N)* on individual sites. a, A general diagram consists of n_j boxes arranged into at most two columns (to satisfy fermionic antisymmetry with only two orbital states), with heights denoted by p and q, such that $N \geq p \geq q$ and $p+q=n_j$. See Supplementary Information for a brief review of Young diagrams. **b**, The Young diagrams for the two special cases discussed in the main text: (**1**) $(p,q)=(1,0)$ and (**2**) $(p,q)=(p,0)$ on a bipartite lattice.

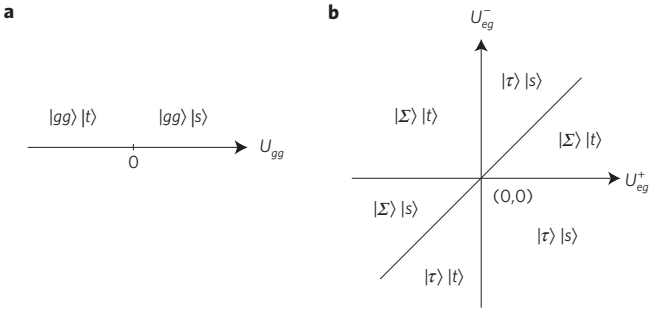

Figure 3 | The ground-state phase diagram for the *SU(N = 2)* Kugel–Khomskii model restricted to two wells, left and right. a, The phase diagram for $T_z=-1$ (two g atoms). $|gg\rangle=|gg\rangle_{LR}$ (L and R denote left and right wells, respectively). $|s\rangle$ and $|t\rangle$ are spin singlet and triplet states, respectively. **b**, The phase diagram for $T_z=0$ (one g atom and one e atom). $|\Sigma\rangle=(1/\sqrt{2})(|eg\rangle_{LR}-|ge\rangle_{LR})$ and $|\tau\rangle=(1/\sqrt{2})(|eg\rangle_{LR}+|ge\rangle_{LR})$ are antisymmetric and symmetric orbital states, respectively. See Supplementary Information for a detailed discussion of both of these diagrams.

One can alternatively implement the two-orbital Hubbard model with two ground-state species of alkaline-earth atoms (for example, ^{171}Yb and ^{173}Yb or ^{173}Yb and ^{87}Sr). If we still refer to them as $|g\rangle$ and $|e\rangle$, the nuclear distinguishability and the fact that both atoms are in the ground state will result in $a_{eg}^{+}=a_{eg}^{-}$, corresponding to an enhanced symmetry (see Methods). Although experimentally more challenging, the use of two different ground-state species will solve the problem of losses associated with collisions of two excited state atoms and will reduce the (already very weak) nuclear-spin dependence of a_{ee} and a_{eg}.

Spin Hamiltonians

One of the simplest interesting limits of equation (2) is the strongly interacting regime ($J/U \ll 1$) where the Hilbert space is restricted to a given energy manifold of the $J_g = J_e = 0$ Hamiltonian (with a fixed number of atoms on each site), and tunnelling is allowed only virtually, giving rise to an effective spin (and pseudo-spin) Hamiltonian. Single-site energy manifolds can be classified according to the number of atoms $n_j = n_{jg} + n_{je}$, the pseudo-spin component T_j^z and the spin symmetry ($SU(N)$ representation) described by a Young diagram. As shown in Fig. 2a, each diagram consists of n_j boxes and at most two columns of heights p and q, representing two sets of antisymmetrized indices.

The $U(1)\times SU(N)$ symmetry of equation (2) restricts the order J^2 spin Hamiltonian to the form

$$\begin{aligned} H_{(p,q)} = & \sum_{\langle i,j\rangle,\alpha}\left[\kappa_\alpha^{ij} n_{i\alpha} n_{j\alpha} + \lambda_\alpha^{ij} S_m^n(i,\alpha) S_n^m(j,\alpha)\right] \\ & + \sum_{\langle i,j\rangle}\Big[\kappa_{ge}^{ij} n_{ig} n_{je} + \lambda_{ge}^{ij} S_m^n(i,g) S_n^m(j,e) \\ & + \tilde{\kappa}_{ge}^{ij} S_{gm}^{em}(i) S_{en}^{gn}(j) + \tilde{\lambda}_{ge}^{ij} S_{gm}^{en}(i) S_{en}^{gm}(j) + \{i \leftrightarrow j\}\Big] \end{aligned} \quad (3)$$

where the sum over n and m is implied in all but the κ terms and $S_{\beta n}^{\alpha m}(j) = c_{j\beta n}^{\dagger} c_{j\alpha m}$. $\{i \leftrightarrow j\}$ means that all four preceding terms are repeated with i and j exchanged. The coefficients κ, λ, $\tilde{\kappa}$ and $\tilde{\lambda}$ are of order J^2/U with the exact form determined by what single-site energy manifolds we are considering. κ terms describe nearest-neighbour repulsion or attraction, and λ, $\tilde{\kappa}$ and $\tilde{\lambda}$ terms describe nearest-neighbour exchange of spins, pseudo-spins and complete atomic states, respectively. Without loss of generality, $\kappa_\alpha^{ij} = \kappa_\alpha^{ji}$ and $\lambda_\alpha^{ij} = \lambda_\alpha^{ji}$. In many cases (for example, case (2) below), the Hilbert space, which $H_{(p,q)}$ acts on, has n_{ie} and n_{ig} constant for all i, which not only forces $\tilde{\kappa}_{ge}^{ij} = \tilde{\lambda}_{ge}^{ij} = 0$ but also enables one to ignore the constant κ_α^{ij} and κ_{ge}^{ij} terms. We now discuss two special cases of $H_{(p,q)}$ shown in Fig. 2b. A third case, $(p,q)=(1,1)$, which reduces for $N=2$ to the spin-1 Heisenberg antiferromagnet, is discussed in the Supplementary Information.

(1) In the case of one atom per site, $(p,q)=(1,0)$. $H_{(p,q)}$ is then a generalization to arbitrary N of the $SU(N=2)$ Kugel–Khomskii model[9,13], and we rewrite it as (see Supplementary Information)

$$\begin{aligned} H_{(1,0)} = & \sum_{\langle i,j\rangle}\Big[2(\tilde{\kappa}_{ge}+\tilde{\lambda}_{ge}S_{ij}^2)(T_i^x T_j^x + T_i^y T_j^y) + \lambda_{ge} S_{ij}^2 + \kappa_{ge} \\ & -[A+BS_{ij}^2]\left(T_i^z T_j^z + \frac{1}{4}\right) + h(1-S_{ij}^2)(T_i^z + T_j^z)\Big] \end{aligned} \quad (4)$$

where $S_{ij}^2 = \sum_{mn} S_m^n(i) S_n^m(j)$ is $+1$ (-1) for a symmetric (antisymmetric) spin state, $A = 2\kappa_{ge} - \kappa_e - \kappa_g$, $B = 2\lambda_{ge} - \lambda_e - \lambda_g$ and $h = (\kappa_e - \kappa_g)/2 = (\lambda_g - \lambda_e)/2$. The $N=2$ Kugel–Khomskii Hamiltonian is used to model the spin–orbital interactions (not to be confused with relativistic spin–orbit coupling) in transition-metal oxides with the perovskite structure[13]. Our implementation enables us to realize clean spin–orbital interactions unaltered by lattice and Jahn–Teller distortions present in solids[13].

To get a sense of the competing spin and orbital orders[10–12] characterizing $H_{(1,0)}$, we consider the simplest case of only two sites (L and R) and $N=2$ (with spin states denoted by $\uparrow$ and $\downarrow$). To avoid losses in e–e collisions, we set $U_{ee}=\infty$ (see Supplementary Information). The double-well ground-state phase diagram for $T^z=1$ (two e atoms) is then trivial; the $T^z=-1$ (two g atoms) and $T^z=0$ (one g atom and one e atom) diagrams are shown in Fig. 3. One can see that, depending on the signs and relative magnitudes of the interactions, various combinations of ferromagnetic (triplet) and antiferromagnetic (singlet) spin and orbital orders are favoured. In the Methods section, we propose a double-well experiment along the lines of ref. 39 to probe the spin–orbital interactions giving rise to the $T^z=0$ diagram in Fig. 3b. Multi-well extensions of this experiment may shed light on the model's many-body phase diagram, which has been studied for $N=2$ and mostly at the mean-field level or in special cases, such as in one dimension (1D) or in the presence of enhanced symmetries (see for example, refs 10–12).

(2) To study $SU(N)$ spin physics alone, we consider the case of only g atoms. On a bipartite lattice with sublattices A and B, we choose A sites to have $n_A < N$ atoms $[(p,q)=(n_A,0)]$ and B sites to have $n_B < N$ atoms $[(p,q)=(n_B,0)]$. This set-up can be

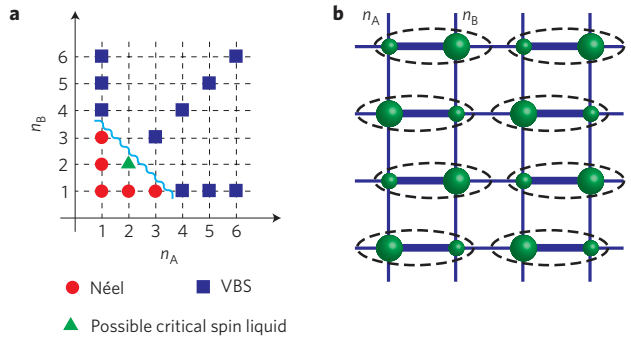

Figure 4 | Probing the phases of the *SU(N)* antiferromagnet on a 2D square lattice. a, The phase diagram for the case $n_A + n_B = N$. Some points on this diagram have been explored in earlier numerical studies[29–31] and are marked according to the ground state obtained: Néel (circles), columnar VBS (shown schematically in **b**) (squares) and possibly critical spin liquid (triangle)[30,31]. As for sufficiently large N quantum fluctuations tend to destabilize long-range magnetic ordering, it is likely that VBS ordering characterizes the ground state for all $N > 4$ (that is, above the wavy line). **b**, Thick bonds connect spins that are more strongly correlated than spins connected by thin bonds, and dashed lines encircle (approximate) *SU(N)* singlets.

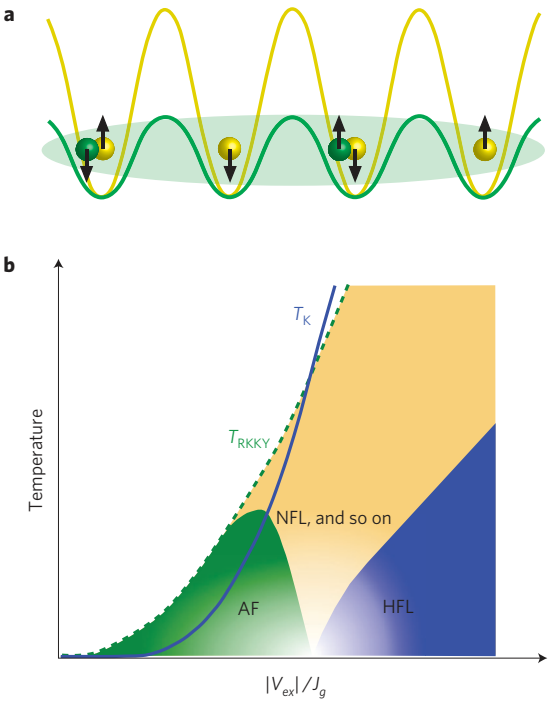

Figure 5 | KLM for the case $N = 2$. a, Schematic of the set-up. *g* atoms are green; *e* atoms are yellow; the spin basis is $\{\uparrow, \downarrow\}$. **b**, Schematic representation of the competition between RKKY magnetism versus Kondo singlet formation in the *SU*(2) antiferromagnetic (AF) KLM (see refs 16, 25, 26 and references therein). In this model, the localized spin-1/2 *e* atoms couple antiferromagnetically to the delocalized *g* atoms through an onsite exchange interaction proportional to V_{ex}. This coupling favours the formation of localized Kondo singlets between *e* and *g* atoms, with characteristic energy scale $k_B T_K \sim J_g \exp(-cJ_g/|V_{ex}|)$, with c being a dimensionless constant of order one[25]. On the other hand, the *g* atoms can mediate long-range RKKY interactions between the *e* atoms, giving rise to magnetic order (which can be antiferromagnetic or ferromagnetic depending on the density of *g* atoms), where the characteristic energy is $k_B T_{RKKY} \sim V_{ex}^2/J_g$. The competition between the Kondo effect and RKKY magnetism leads to very rich physics. For small values of $|V_{ex}|/J_g$, the RKKY interaction is dominant and the system orders magnetically. At intermediate values of $|V_{ex}|/J_g$, the energy scales T_K and T_{RKKY} are of comparable strength, and a variety of new quantum phenomena are expected to arise, including quantum criticality and non-Fermi liquid (NFL) physics[25,26]. With a further increase of the $|V_{ex}|/J_g$ coupling, magnetic order is suppressed, the localized *e* atoms become screened into singlet states and melt into the *g*-atom Fermi sea, forming the so-called HFL state. The large Fermi volume[21], which is set by the total number of *g* atoms plus *e* atoms, can be directly probed by measuring the momentum distribution by means of time-of-flight imaging.

engineered in cold atoms by using a superlattice to adjust the depths of the two sublattices favouring a higher filling factor in deeper wells. $H_{(p,q)}$ then reduces to

$$H_{(p,0)} = \frac{2J_g^2 U_{gg}}{U_{gg}^2 - (U_{gg}(n_A - n_B) + \Delta)^2} \sum_{\langle i,j \rangle} S_{ij}^2 \qquad (5)$$

where Δ is the energy offset between adjacent lattice sites. The coupling constant can be made either positive (antiferromagnetic) or negative (ferromagnetic) depending on the choice of parameters[39]. Three-body recombination processes will probably limit the lifetime of the atoms when $n_j \geq 3$ (see Supplementary Information).

We focus on the 2D square lattice in the antiferromagnetic regime. The case $n_A + n_B = N$ shares with the $SU(2)$ Heisenberg model the crucial property that two adjacent spins can form an $SU(N)$ singlet, and has thus been studied extensively as a large-N generalization of $SU(2)$ magnetism[27,28]. Figure 4a shows the expected phase diagram for the case $n_A + n_B = N$, which features Néel (circles), VBS (squares) (Fig. 4b) and possible critical spin-liquid (triangle)[30,31] ground states. To access various ground states of the system, the initial state must be carefully prepared so that the conserved quantities S_m^m take values appropriate for these ground states. Another interesting and experimentally relevant case, $n_A = n_B \neq N/2$, which can also show spin-liquid and VBS-type ground states, is discussed in the Supplementary Information and in ref. 34.

As one can vary N just by choosing the number of initially populated Zeeman levels (for example, through a combination of optical pumping and coherent manipulation), alkaline-earth atoms offer a unique arena to probe the phase diagram of $H_{(p,0)}$, including exotic phases such as VBS (Fig. 4b), as well as competing magnetically ordered states. We propose to load a band insulator of N *g* atoms per site, then slowly split each well into two to form an array of independent $SU(N)$ singlets in a pattern shown in Fig. 4b. The intersinglet tunnelling rate should then be adiabatically increased up to the intrasinglet tunnelling rate. As N increases, the magnetic or singlet nature of the state can be probed by measuring the Néel order parameter (see the description of the Kugel–Khomskii double-well experiment in the Methods section) and spin–spin correlations by means of noise spectroscopy in the time-of-flight[40] (which directly measures $\sum_{j,k} \langle S_n^m(j,g) S_m^n(k,g) \rangle e^{iQ(j-k)}$).

The Kondo lattice model (KLM)

The $SU(N)$ KLM (refs 15, 17) is another example of the rich physics, beyond the Mott regime, that could be simulated with alkaline-earth atoms. The KLM is one of the canonical models used to study strongly correlated electron systems, such as manganese oxide perovskites[20] and rare-earth and actinide compounds classed as heavy-fermion materials[25].

For its implementation with cold atoms (for $N = 2$, see also refs 23, 24), we propose to put one *e* atom (localized spin) per site in a deep lattice such that $J_e \ll U_{ee}$, so that we can set $J_e = 0$ and

$n_{je}=1$ for all j in equation (2). We also suppose that we can set $U_{gg}=0$, for example, by taking a very shallow g lattice (see Fig. 5a). The resulting Hamiltonian is the $SU(N)$ KLM (refs 15, 17)

$$H_{\mathrm{KLM}} = -\sum_{\langle j,i\rangle m} J_g (c^{\dagger}_{igm} c_{jgm} + \mathrm{h.c.}) + V_{ex} \sum_{j,m,m'} c^{\dagger}_{jgm} c^{\dagger}_{jem'} c_{jgm'} c_{jem} \quad (6)$$

The magnitude of V_{ex} can be adjusted by shifting the e and g lattices relative to each other[7].

The properties of the $SU(N)$ KLM depend crucially on the sign of the exchange interaction. For concreteness, we focus on the antiferromagnetic case ($V_{ex}<0$), which favours formation of spin-antisymmetric states (singlets, for $N=2$) between mobile fermions and localized spins. This regime describes the physics of heavy-fermion materials[25], and, in the case of a single localized spin, gives rise to the Kondo effect.

In the limit $|V_{ex}| \ll J_g, g$ atoms mediate long-range Ruderman–Kittel–Kasuya–Yosida (RKKY) interactions[14] between localized spins and tend to induce magnetic ordering (antiferromagnetic or ferromagnetic depending on the density of g atoms) of these spins, at least for $N=2$. The engineering of RKKY interactions can be tested in an array of isolated double wells (see the Methods section). At intermediate and large $|V_{ex}|$, the formation of Kondo singlets dominates the RKKY interaction and favours a magnetically disordered heavy-Fermi-liquid (HFL) ground state with a significantly enhanced effective quasiparticle mass (see Fig. 5b). The competition between RKKY interactions and the Kondo effect in the regime where both are comparable is subtle, and the resulting phases and phase transitions[25,26] are not well understood. Ultracold alkaline-earth atoms provide a promising platform to study these phases and phase transitions.

In the large-N limit[15,17], the $SU(N)$ HFL can be controllably studied, and $1/N$ expansions have successfully reproduced the experimentally observed properties of the HFL. However, very little is known about the $SU(N)$ model outside the HFL regime. Several very interesting parameter regimes in this domain can be directly probed with our system, as discussed in the Methods section.

Experimental accessibility

The phenomena described in this article can be probed with experimental systems under development. Indeed, we show in the Methods section that $SU(N)$-breaking terms are sufficiently weak, and here we discuss the temperature requirements.

The key energy scale in the spin Hamiltonians (3) is the superexchange energy J^2/U, whereas the RKKY energy scale is $k_{\mathrm{B}}T_{\mathrm{RKKY}} \sim V_{ex}^2/J_g$. In their region of validity ($J<U$ and $|V_{ex}|<J_g$, respectively), these energy scales are limited from above by the interaction energy (U and $|V_{ex}|$, respectively), which typically corresponds to temperatures $T \lesssim 100\,\mathrm{nK}$ (ref. 39). Owing to the extra cooling associated with certain adiabatic changes[41,42], $T \sim 10\,\mathrm{nK}$ and the Mott insulating regime have already been achieved with fermionic alkali atoms[43], and are therefore expected to be achievable with fermionic alkaline earths, as well (a bosonic alkaline-earth Mott insulator has already been achieved[44]). Furthermore, the requirement to reach $k_{\mathrm{B}}T$ smaller than J^2/U or V_{ex}^2/J_g can often be relaxed. First, the double-well experiments, such as the ones discussed in the Methods section in the contexts of the Kugel–Khomskii model and the KLM, are done out of thermal equilibrium, and can, thus, access energy scales far below the temperature of the original cloud[39]. Second, for $SU(N)$ antiferromagnets, the energy range between J^2/U and NJ^2/U may also show intriguing physics: in this regime, $SU(N)$ singlets, which require NJ^2/U energy to break, stay intact but can diffuse around. Finally, in the $V_{ex}<0$ KLM, exotic heavy-Fermi-liquid behaviour is expected when $J_g \lesssim |V_{ex}|$ and the temperature is below the Kondo temperature, that is, $k_{\mathrm{B}}T \lesssim J_g \exp(-cJ_g/|V_{ex}|)$ where c is a dimensionless constant of order one[25]. Thus, with J_g chosen to be of the order of $|V_{ex}|$, $k_{\mathrm{B}}T$ as high as $\sim|V_{ex}|$ may be sufficient.

Outlook

The proposed experiments should be regarded as bridges aiming to connect well-understood physics to the complex and poorly understood behaviour of strongly correlated systems. It is important to emphasize that, except for the 1D case, the phase diagram of most of the models considered is known only at the mean-field level or numerically in reduced system sizes. Therefore, their experimental realization in clean and controllable ultracold atomic systems can provide significant advances.

Our proposal motivates other new lines of research. Ultracold bosonic or fermionic diatomic molecules[45] may give rise to similar $SU(N)$ models with large N and with the possibility of long-range interactions. Ions with alkaline-earth-like structure, such as Al^+ could also be considered in this context. It would also be interesting to explore the possibility of realizing topological phases with $SU(N)$ models for applications in topological quantum computation[34]. Beyond quantum magnetism, the fact that the formation of $SU(N)$ singlets requires N partners might give rise to exotic types of superfluidity and new types of Bardeen–Cooper–Schrieffer/Bose–Einstein-condensation (BCS-BEC) crossover[37]. Practical applications of our Hubbard model, such as the calculation of the collisional frequency shift in atomic clocks[46], can also be foreseen.

Note added in proof: After the submission of this article, a theoretical study of the $SU(6)$-symmetric ^{173}Yb system was reported[47].

Methods

Experimental tools available for alkaline-earth atoms. Many experimental tools, such as tuning the interaction strength by adjusting laser intensities[39], are common to both alkali and alkaline-earth atoms. There are, however, some experimental tools specific to alkaline earths; we review them in this section.

First, a combination of optical pumping[2] and direct coherent manipulation of the $|g\rangle-|e\rangle$ transition in the presence of a magnetic field[1,2] can be used[8] to prepare any desired single-atom state within the $2(2I+1)$-dimensional manifold with basis $|\alpha m\rangle$, where $\alpha=g$ or e and $m=-I,\ldots,I$. This coherent manipulation can also be used to exchange quantum information between nuclear spin states and electronic states. Second, by using far-detuned probe light or a large magnetic field to decouple the electronic angular momentum J and the nuclear spin I, the electronic $|g\rangle-|e\rangle$ degree of freedom can be measured by collecting fluorescence without destroying the nuclear spin state[5,8]. Fluorescence measurement of the nuclear spins can be achieved by mapping nuclear spin states onto electronic states[7,8]: for example, for a spin-1/2 nucleus, a π pulse between $|g,m=1/2\rangle$ and $|e,m=-1/2\rangle$ enables one to accomplish a swap gate between the nuclear $\{1/2,-1/2\}$ qubit and the electronic $\{e,g\}$ qubit. Single-site spatial resolution during the coherent manipulation and fluorescence measurement can be achieved using magnetic field gradients[7] or dark-state-based techniques[8,48] that rely on an auxiliary laser field for which the intensity vanishes at certain locations. Third, an appropriate choice of laser frequencies enables one to obtain independent lattices for states g and e (ref. 7). Finally, optical Feshbach resonances[49] may be used to control scattering lengths site-specifically and nearly instantaneously.

Enhanced symmetries. Whereas in the general case, our Hubbard model (equation (2)) satisfies $U(1)\times \mathrm{SU}(N)$ symmetry, for particular choices of parameters, higher symmetry is possible. In particular, if $J_g=J_e$ and the interaction energies for all states within the pseudo-spin triplet are equal ($U_{gg}=U_{ee}=U_{eg}^{+}$), the full $SU(2)$ symmetry (not just $U(1)$) in the pseudo-spin space is satisfied. Alternatively, if $V_{ex}=0$, then both $S_n^m(i,g)$ and $S_n^m(i,e)$ generate $SU(N)$ symmetries resulting in the overall $U(1)\times SU(N)\times SU(N)$ symmetry. Finally, if both conditions are satisfied, that is, all four U_X are equal and $J_g=J_e$, then H satisfies the full $SU(2N)$ symmetry ($2N$ can be as high as 20) generated by

$$S^{\alpha m}_{\beta n} = \sum_j S^{\alpha m}_{\beta n}(j) = \sum_j c^{\dagger}_{j\beta n} c_{j\alpha m}$$

in which case the interaction reduces to $\frac{U}{2}\sum_j n_j(n_j-1)$, where $n_j=n_{jg}+n_{je}$.

In the case when $|e\rangle$ and $|g\rangle$ correspond to two ground states of two different atoms (with nuclear spin I_e and I_g, respectively), we will have $a_{eg}^{+}=a_{eg}^{-}$ (that is, $V_{ex}=0$), which is equivalent to imposing $U(1)\times SU(N_g=2I_g+1)\times SU(N_e=2I_e+1)$ symmetry, where $SU(2I_\alpha+1)$ is generated by $S_n^m(i,\alpha)$. Whereas for $I_g\neq I_e$, the m index in $c_{j\alpha m}$ will run over a

different set of values depending on α, the Hubbard Hamiltonian will still have the form of equation (2) (except with $V_{ex}=0$). If one further assumes that $J_g=J_e$ and $U_{gg}=U_{ee}=U_{eg}$, the interaction satisfies the full $SU(N_g+N_e)$ symmetry. It is worth noting that for the case of two different ground-state atoms, this higher symmetry is easier to achieve than for the case of two internal states of the same atom, because $a_{eg}^{+}=a_{eg}^{-}$ automatically. Thus, in particular, it might be possible to obtain $SU(18)$ with ^{87}Sr ($I=9/2$) and ^{43}Ca ($I=7/2$) simply by adjusting the intensities of the two lattices (to set $J_g=J_e$ and $U_{gg}=U_{ee}$) and then shifting the two lattices relative to each other (to set $U_{eg}=U_{gg}$).

Enhanced symmetries of the Hubbard model (equation (2)) are inherited by the spin Hamiltonian (equation (3)). In particular, imposing $SU(2)\times SU(N)$ instead of $U(1)\times SU(N)$ forces $\kappa_{ge}^{ij}=\kappa_{ge}^{ji}$, $\tilde{\kappa}_{ge}^{ij}=\tilde{\kappa}_{ge}^{ji}$, $\kappa_{g}^{ij}=\kappa_{e}^{ij}=\kappa_{ge}^{ij}+\tilde{\kappa}_{ge}^{ij}\equiv\kappa^{ij}$, $\lambda_{ge}^{ij}=\lambda_{ge}^{ji}$, $\tilde{\lambda}_{ge}^{ij}=\tilde{\lambda}_{ge}^{ji}$, $\lambda_{g}^{ij}=\lambda_{e}^{ij}=\lambda_{ge}^{ij}+\tilde{\lambda}_{ge}^{ij}\equiv\lambda^{ij}$. Alternatively, imposing $U(1)\times SU(N)\times SU(N)$ forces $\tilde{\kappa}_{ge}^{ij}=\lambda_{ge}^{ij}=0$. Finally, imposing the full $SU(2N)$ forces the satisfaction of both sets of conditions, yielding

$$H=\sum_{\langle i,j\rangle}\left[\kappa^{ij}n_in_j+\lambda^{ij}S_{\alpha m}^{\beta n}(i)S_{\beta n}^{\alpha m}(j)\right]$$

which is, of course, equivalent to restricting equation (3) to g atoms alone and extending labels m and n to run over $2N$ states instead of N.

Double-well Kugel–Khomskii and RKKY experiments. In the main text and in the following section, we discuss the open questions and previously unexplored regimes associated with the $SU(N)$ Kugel–Khomskii model and the KLM that can be studied with ultracold alkaline-earth atoms. As a stepping stone towards these many-body experiments, we propose in this section two proof-of-principle experiments in an array of isolated double wells with $N=2$ (with the spin basis $\{\uparrow,\downarrow\}$): one to probe the spin–orbital interactions of the Kugel–Khomskii model and one to probe the RKKY interactions associated with the KLM.

We first propose an experiment along the lines of ref. 39 to probe the spin–orbital interactions giving rise to the $T^z=0$ diagram in Fig. 3b. In the Supplementary Information, we describe how to prepare an array of independent double wells in the state $|e,\uparrow\rangle_L|g,\downarrow\rangle_R$, which is a superposition of the four eigenstates featured in Fig. 3b. The energies of these four eigenstates (Supplementary Equations (S4)–(S7)) can be extracted from the Fourier analysis of the population imbalance as a function of time: $\Delta N(t)=n_{eR}+n_{gL}-n_{gR}-n_{eL}=-\cos[(4tJ_e/\hbar U_{eg}^{-})]-\cos[(4tJ_e/\hbar U_{eg}^{+})]$. ΔN can be measured by combining the dumping technique, band mapping and Stern–Gerlach filtering of ref. 39 with the use of two probe laser frequencies to distinguish between $|g\rangle$ and $|e\rangle$.

We now turn to the double-well experiment aimed at probing RKKY interactions. After preparing the state $(1/\sqrt{2})(|g,\downarrow\rangle_L+|g,\downarrow\rangle_R)|e,\downarrow\rangle_L|e,\uparrow\rangle_R$ (see Supplementary Information for how to prepare this state), we propose to monitor the Néel order parameter for the e atoms, $N_{ez}=(1/2)[n_{e\uparrow L}-n_{e\downarrow L}-(n_{e\uparrow R}-n_{e\downarrow R})]$. In the limit $|V_{ex}|\ll J_g$, $N_{ez}(t)=-(1/3)\cos(V_{ex}t/\hbar)-(2/3)\cos((V_{ex}t/2\hbar)-(3V_{ex}^2t/8J_g\hbar))$ (in the Supplementary Information, we present the plot of $N_{ez}(t)$ for $V_{ex}=-J_g/10$). It shows fast oscillations with frequency $\sim V_{ex}$, modulated by an envelope of frequency $\sim V_{ex}^2/J_g$ induced by RKKY interactions. To probe only RKKY interactions, it is important to suppress superexchange $\sim J_e^2/U_{ee}$ and thus to choose J_e/U_{ee} small. To study the full spatial dependence of RKKY interactions, one must of course go beyond the double-well set-up. We also note that recent experiments using alkali atoms populating the lowest two vibrational levels of a deep optical lattice have measured the local singlet-triplet splitting induced by V_{ex} (ref. 50).

Physics accessible with the alkaline-earth KLM. The alkaline-earth atom realization of the antiferromagnetic KLM is well suited to access a number of parameter regimes that are out of reach in solid-state materials. One example is the 1D limit, because, to our knowledge, real solid-state materials showing KLM physics are restricted to 2D or 3D. Another example is the regime of large Kondo exchange ($|V_{ex}|\gg J_g$), which is interesting even for $N=2$. In this limit, the system is well described by the $U\to\infty$ Hubbard model[18] by identifying the Kondo singlets with empty sites (holes) and the unpaired localized spins with hard-core electrons. From this mapping, possible ferromagnetic ordering is expected at a small hole concentration (small n_g); however, the stability of this phase for increasing hole concentration and finite $|V_{ex}|$ values remains unknown. For general N, in the extreme limit $J_g=0$, the ground state is highly degenerate: for any distribution of the g-atom density $n_{ig}<N$, there is a ground state (with further spin degeneracy), where on each site the spins combine antisymmetrically to minimize the exchange interaction. Lifting of such extensive degeneracies often leads to exotic ground states; this will be addressed in future studies using degenerate perturbation theory in J_g/V_{ex}. For $N>2$, antiferromagnetic $SU(N)$ spin models have a different kind of extensive degeneracy, which was argued to destroy antiferromagnetism and to lead to non-magnetic spin-liquid and VBS-like ground states[34]. Similar expectations are likely to apply to the KLM at small $|V_{ex}|/J_g$, where the $N=2$ antiferromagnetism may give way to situations where the localized spins form a non-magnetic state that is effectively decoupled from the mobile fermions[22].

Even though we have set U_{gg} to zero in equation (6), it can be tuned, for example, by adjusting the g-lattice depth and can give rise to interesting physics. For example, the $n_g=1$ case, which is known to be for $N=2$ either an antiferromagnetic insulator or a Kondo insulator depending on the ratio $|V_{ex}|/J_g$ (ref. 19), will become for large enough U_{gg} and $N>2$ a Mott insulator, because the two atoms on each site cannot combine to form an $SU(N)$ singlet. If n_g is reduced from unity, the doping of this Mott insulator can be studied, and it will be interesting to understand how this physics, usually associated with cuprate superconductors, is related to the other ground states of the KLM, usually associated with heavy-fermion compounds.

Experimental accessibility. Immediate experimental accessibility makes our proposal particularly appealing. Having shown in the main text that the temperature requirements of our proposal are within reach of present experimental systems, here we show that the nuclear-spin dependence of interaction energies is sufficiently weak to keep the $SU(N)$ physics intact.

In the Supplementary Information, nuclear-spin-dependent variation in the interaction energies is estimated to be $\Delta U_{gg}/U_{gg}\sim 10^{-9}$ and $\Delta U_{ee}/U_{ee}\sim\Delta U_{eg}^{\pm}/U_{eg}^{\pm}\sim 10^{-3}$. As the scale of $SU(N)$ breaking is at most ΔU, a very conservative condition for the physics to be unaffected by $SU(N)$ breaking is that all important energy scales are greater than ΔU. In particular, in the spin models with more than one atom per site, the condition is $\Delta U\ll J^2/U$, which can be satisfied simultaneously with $J\ll U$ even for $\Delta U/U\sim 10^{-3}$. With one atom per site, the $SU(N)$ breaking scale is not ΔU but rather $(J/U)^2\Delta U$, which relaxes the condition to the immediately satisfied $\Delta U/U\ll 1$. Similarly, in the KLM, the conditions $\Delta V_{ex}\ll J,|V_{ex}|$ can be satisfied for $\Delta V_{ex}/|V_{ex}|\sim 10^{-3}$.

Received 18 May 2009; accepted 26 January 2010; published online 28 February 2010

References

1. Boyd, M. M. *et al.* Nuclear spin effects in optical lattice clocks. *Phys. Rev. A* **76,** 022510 (2007).
2. Campbell, G. K. *et al.* Probing interactions between ultracold fermions. *Science* **324,** 360–363 (2009).
3. Lemke, N. D. *et al.* Spin-1/2 optical lattice clock. *Phys. Rev. Lett.* **103,** 063001 (2009).
4. Fukuhara, T., Takasu, Y., Kumakura, M. & Takahashi, Y. Degenerate fermi gases of ytterbium. *Phys. Rev. Lett.* **98,** 030401 (2007).
5. Reichenbach, I. & Deutsch, I. H. Sideband cooling while preserving coherences in the nuclear spin state in group-II-like atoms. *Phys. Rev. Lett.* **99,** 123001 (2007).
6. Hayes, D., Julienne, P. S. & Deutsch, I. H. Quantum logic via the exchange blockade in ultracold collisions. *Phys. Rev. Lett.* **98,** 070501 (2007).
7. Daley, A. J., Boyd, M. M., Ye, J. & Zoller, P. Quantum computing with alkaline-earth-metal atoms. *Phys. Rev. Lett.* **101,** 170504 (2008).
8. Gorshkov, A. V. *et al.* Alkaline-earth-metal atoms as few-qubit quantum registers. *Phys. Rev. Lett.* **102,** 110503 (2009).
9. Kugel, K. I. & Khomskii, D. I. Crystal structure and magnetic properties of substances with orbital degeneracy. *Sov. Phys. JETP* **37,** 725–730 (1973).
10. Arovas, D. P. & Auerbach, A. Tetrahis(dimethylamino)ethylene-C_{60}: Multicomponent superexchange and Mott ferromagnetism. *Phys. Rev. B* **52,** 10114–10121 (1995).
11. Li, Y. Q., Ma, M., Shi, D. N. & Zhang, F. C. $SU(4)$ theory for spin systems with orbital degeneracy. *Phys. Rev. Lett.* **81,** 3527–3530 (1998).
12. Pati, S. K., Singh, R. R. P. & Khomskii, D. I. Alternating spin and orbital dimerization and spin-gap formation in coupled spin–orbital systems. *Phys. Rev. Lett.* **81,** 5406–5409 (1998).
13. Tokura, Y. & Nagaosa, N. Orbital physics in transition-metal oxides. *Science* **288,** 462–468 (2000).
14. Ruderman, M. A. & Kittel, C. Indirect exchange coupling of nuclear magnetic moments by conduction electrons. *Phys. Rev.* **96,** 99–102 (1954).
15. Coqblin, B. & Schrieffer, J. R. Exchange interaction in alloys with cerium impurities. *Phys. Rev.* **185,** 847–853 (1969).
16. Doniach, S. The Kondo lattice and weak antiferromagnetism. *Physica* B+C **91,** 231–234 (1977).
17. Coleman, P. $1/N$ expansion for the Kondo lattice. *Phys. Rev. B* **28,** 5255–5262 (1983).
18. Tsunetsugu, H., Sigrist, M. & Ueda, K. The ground-state phase diagram of the one-dimensional Kondo lattice model. *Rev. Mod. Phys.* **69,** 809–863 (1997).
19. Assaad, F. F. Quantum Monte Carlo simulations of the half-filled two-dimensional Kondo lattice model. *Phys. Rev. Lett.* **83,** 796–799 (1999).
20. Tokura, Y. (ed.) *Colossal Magnetoresistive Oxides* (Gordon and Breach, 2000).
21. Oshikawa, M. Topological approach to Luttinger's theorem and the Fermi surface of a Kondo lattice. *Phys. Rev. Lett.* **84,** 3370–3373 (2000).
22. Senthil, T., Sachdev, S. & Vojta, M. Fractionalized Fermi liquids. *Phys. Rev. Lett.* **90,** 216403 (2003).
23. Duan, L.-M. Controlling ultracold atoms in multi-band optical lattices for simulation of Kondo physics. *Europhys. Lett.* **67,** 721–727 (2004).
24. Paredes, B., Tejedor, C. & Cirac, J. I. Fermionic atoms in optical superlattices. *Phys. Rev. A.* **71,** 063608 (2005).

25. Coleman, P. in *Handbook of Magnetism and Advanced Magnetic Materials* Vol. 1 (eds Kronmüller, H. & Parkin, S.) 95–148 (Wiley, 2007).
26. Gegenwart, P., Si, Q. & Steglich, F. Quantum criticality in heavy-fermion metals. *Nature Phys.* **4,** 186–197 (2008).
27. Read, N. & Sachdev, S. Valence-bond and spin-Peierls ground states of low-dimensional quantum antiferromagnets. *Phys. Rev. Lett.* **62,** 1694–1967 (1989).
28. Marston, J. B. & Affleck, I. Large-*n* limit of the Hubbard–Heisenberg model. *Phys. Rev. B* **39,** 11538–11558 (1989).
29. Harada, K., Kawashima, N. & Troyer, M. Néel and spin-Peierls ground states of two-dimensional *SU(N)* quantum antiferromagnets. *Phys. Rev. Lett.* **90,** 117203 (2003).
30. Assaad, F. F. Phase diagram of the half-filled two-dimensional *SU(N)* Hubbard–Heisenberg model: A quantum Monte Carlo study. *Phys. Rev. B* **71,** 075103 (2005).
31. Paramekanti, A. & Marston, J. B. *SU(N)* quantum spin models: a variational wavefunction study. *J. Phys. Condens. Matter* **19,** 125215 (2007).
32. Greiter, M. & Rachel, S. Valence bond solids for *SU(n)* spin chains: Exact models, spinon confinement, and the Haldane gap. *Phys. Rev. B* **75,** 184441 (2007).
33. Xu, C. & Wu, C. Resonating plaquette phases in *SU*(4) Heisenberg antiferromagnet. *Phys. Rev. B* **77,** 134449 (2008).
34. Hermele, M., Gurarie, V. & Rey, A. M. Mott insulators of ultracold fermionic alkaline earth atoms: Underconstrained magnetism and chiral spin liquid. *Phys. Rev. Lett.* **103,** 135301 (2009).
35. Wu, C., Hu, J. P. & Zhang, S. C. Exact SO(5) symmetry in the spin-3/2 fermionic system. *Phys. Rev. Lett.* **91,** 186402 (2003).
36. Honerkamp, C. & Hofstetter, W. Ultracold fermions and the *SU(N)* Hubbard model. *Phys. Rev. Lett.* **92,** 170403 (2004).
37. Rapp, A., Hofstetter, W. & Zarand, G. Trionic phase of ultracold fermions in an optical lattice: A variational study. *Phys. Rev. B* **77,** 144520 (2008).
38. Affleck, I., Arovas, D. P., Marston, J. B. & Rabson, D. A. *SU*(2*n*) quantum antiferromagnets with exact C-breaking ground states. *Nucl. Phys. B* **366,** 467–506 (1991).
39. Trotzky, S. *et al.* Time-resolved observation and control of superexchange interactions with ultracold atoms in optical lattices. *Science* **319,** 295–299 (2008).
40. Altman, E., Demler, E. & Lukin, M. D. Probing many-body states of ultracold atoms via noise correlations. *Phys. Rev. A* **70,** 013603 (2004).
41. Hofstetter, W., Cirac, J. I., Zoller, P., Demler, E. & Lukin, M. D. High-temperature superfluidity of fermionic atoms in optical lattices. *Phys. Rev. Lett.* **89,** 220407 (2002).
42. Werner, F., Parcollet, O., Georges, A. & Hassan, S. R. Interaction-induced adiabatic cooling and antiferromagnetism of cold fermions in optical lattices. *Phys. Rev. Lett.* **95,** 056401 (2005).
43. Schneider, U. *et al.* Metallic and insulating phases of repulsively interacting fermions in a 3D optical lattice. *Science* **322,** 1520–1525 (2008).
44. Fukuhara, T., Sugawa, S., Sugimoto, M., Taie, S. & Takahashi, Y. Mott insulator of ultracold alkaline-earth-metal-like atoms. *Phys. Rev. A* **79,** 041604(R) (2009).
45. Ni, K. K. *et al.* A high phase-space-density gas of polar molecules. *Science* **322,** 231–235 (2008).
46. Rey, A. M., Gorshkov, A. V. & Rubbo, C. Many-body treatment of the collisional frequency shift in fermionic atoms. *Phys. Rev. Lett.* **103,** 260402 (2009).
47. Cazalilla, M. A., Ho, A. F. & Ueda, M. Ultracold gases of ytterbium: Ferromagnetism and Mott states in an *SU*(6) Fermi system. *New J. Phys.* **11,** 103033 (2009).
48. Gorshkov, A. V., Jiang, L., Greiner, M., Zoller, P. & Lukin, M. D. Coherent quantum optical control with subwavelength resolution. *Phys. Rev. Lett.* **100,** 093005 (2008).
49. Ciuryło, R., Tiesinga, E. & Julienne, P. S. Optical tuning of the scattering length of cold alkaline-earth-metal atoms. *Phys. Rev. A* **71,** 030701(R) (2005).
50. Anderlini, M. *et al.* Controlled exchange interaction between pairs of neutral atoms in an optical lattice. *Nature* **448,** 452–456 (2007).

Acknowledgements

We gratefully acknowledge conversations with M. M. Boyd, A. J. Daley, S. Fölling, W. S. Bakr, J. I. Gillen, L. Jiang, G. K. Campbell, Y. Qi and N. Blümer. This work was supported by NSF, CUA, DARPA, the Packard Foundation, AFOSR MURI and NIST.

Author contributions

All authors contributed extensively to the work presented in this paper.

Additional information

The authors declare no competing financial interests. Supplementary information accompanies this paper on www.nature.com/naturephysics. Reprints and permissions information is available online at http://npg.nature.com/reprintsandpermissions. Correspondence and requests for materials should be addressed to A.V.G.